

Communication

Five Bonds to Carbon through Tri-Coordination in $\text{Al}_3\text{C}_3^{-/0}$

 Abdul Hamid Malhan ¹, Venkatesan S. Thimmakondur ^{2,*} and Krishnan Thirumoorthy ^{1,*}
¹ Department of Chemistry, School of Advanced Sciences, Vellore Institute of Technology, Vellore 632 014, Tamil Nadu, India; abdulhamid.malhanb2020@vitstudent.ac.in

² Department of Chemistry and Biochemistry, San Diego State University, San Diego, CA 92182-1030, USA

* Correspondence: vthimmakondusamy@sdsu.edu (V.S.T.); thirumoorthy.krishnan@vit.ac.in (K.T.)

Abstract: Here, five bonds to carbon through tri-coordination are theoretically established in the global minimum energy isomers of Al_3C_3^- anion (**1a**) and Al_3C_3 neutral (**1n**) for the first time. Various isomers of $\text{Al}_3\text{C}_3^{-/0}$ are theoretically identified using density functional theory at the PBE0-D3/def2-TZVP level. Chemical bonding features are thoroughly analyzed for these two isomers (**1a** and **1n**) with different bonding and topological quantum chemical tools, such as adaptive natural density partitioning (AdNDP), Wiberg Bond Indices (WBIs), nucleus-independent chemical shifts (NICS), and atoms in molecules (AIM) analyses. The structure of isomer **1a** is planar with C_{2v} symmetry, whereas its neutral counterpart **1n** is non-planar with C_2 symmetry, in which its terminal aluminum atoms are out of the plane. The central allenic carbon atom of isomers **1a** and **1n** exhibits tri-coordination and thus makes it a case of five bonds to carbon, which is confirmed through their total bond order as observed in WBI. Both the isomers show σ - and π -aromaticity and are predicted with the NICS and AdNDP analyses. Further, the results of ab initio molecular dynamics simulations reveal their kinetic stability at room temperature; thus, they are experimentally viable systems.

Keywords: $\text{Al}_3\text{C}_3^{-/0}$; five bonds to carbon; anti-van't Hoff-Le Bel; σ -aromaticity; π -aromaticity; bonding; computational chemistry



Citation: Malhan, A.H.; Thimmakondur, V.S.; Thirumoorthy, K. Five Bonds to Carbon through Tri-Coordination in $\text{Al}_3\text{C}_3^{-/0}$. *Chemistry* **2023**, *5*, 1113–1123. <https://doi.org/10.3390/chemistry5020076>

Academic Editor: Andrea Peluso

Received: 15 April 2023

Revised: 2 May 2023

Accepted: 5 May 2023

Published: 9 May 2023



Copyright: © 2023 by the authors. Licensee MDPI, Basel, Switzerland. This article is an open access article distributed under the terms and conditions of the Creative Commons Attribution (CC BY) license (<https://creativecommons.org/licenses/by/4.0/>).

1. Introduction

The concept of five bonds to carbon became indispensable since the discovery of methanium ion (CH_5^+) in the laboratory in 1950 [1]. Recording the infrared spectra of this simple protonated methane molecule was quite challenging, as it took almost five decades from its discovery [2]. The theoretical investigation of lithium carbides such as CLi_5 and CLi_6 [3] and the experimental realization of CLi_6 through mass spectroscopic measurements further motivated the interest in hyper-coordinate carbon molecules [4]. While computational studies on $\text{Si}_2(\text{CH}_3)_7^+$ [5] and $\text{C}(\text{CH}_3)_5^+$ [6] provided further guidance on hyper-coordinate behavior of group 14 elements, it is the experimental observations such as $[\text{CCH}_3]_6^{2+}$, $\text{HC}[\text{Au}(\text{PPh}_3)]_4^+$, $[(\text{C}_6\text{H}_5)_3\text{PAu}_5\text{C}]^+$, $[(\text{Ph}_3\text{PAu})_6\text{C}]^{2+}$, $\text{C}_6[\text{CH}_3]_6^{2+}$, etc., that gave chemists the real grandeur of hyper-coordinate carbon molecules [7–11]. Akiba and co-workers have shown penta- and hexa-coordinate anthracene moieties through x-ray crystallography and ab initio calculations [12,13]. The iron–molybdenum nitrogenase cofactor existing in diazotrophs is a clear example of hexa-coordinate carbon in biological systems [14]. From the well-known concept of molecules with a planar tetra-coordinate carbon (ptC) atom [15–30], the idea was extended to planar penta-coordinate carbon (ppC) [31–40] and planar hexa-coordinate carbon (phC) [41–44]. Hill and coworkers experimentally reported the existence of a penta-coordinate carbon atom in 1981 [45]. The penta-coordinate carbon atom was also theoretically reported by Gleiter and coworkers [46] in the $\text{Cp}_2\text{Zr}[\text{CH}_2(\text{BH}(\text{C}_6\text{F}_5)_2)]_2$ complex. In 1996, the experimental proof of the first complex with a hyper-coordinate ylidic carbon atom was also reported by Jones and coworkers [47]. While a gradual amount of progress has been made in these classes of molecules to date, to a larger extent in the literature, the concept of making hyper-coordinate carbon molecules was predominantly

focused on making single bonds to the central carbon atom irrespective of whether they are planar or non-planar [48]. However, in this article, the intent is to make five bonds to a carbon atom through tri-coordination instead of penta-coordination, as is normally carried out. To this end, we have theoretically investigated the aluminum–carbon cluster, $\text{Al}_3\text{C}_3^{-/0}$, in both its anion and neutral forms and established the fact that the global minimum isomers (1a and 1n) contain five bonds to carbon through tri-coordination (see Figures 1 and 2).

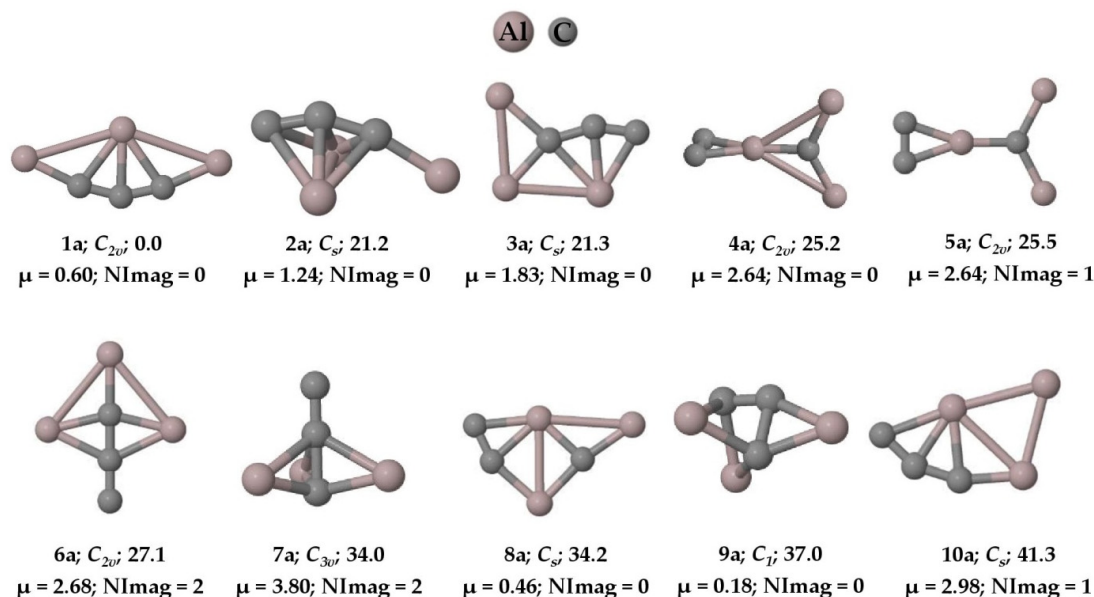


Figure 1. Ten low-lying isomers of Al_3C_3^- with the ZPVE-corrected relative energies (in kcal mol^{-1}), dipole moments (in Debye), and the number of imaginary frequencies (NImag) obtained at the PBE0-D3/def2-TZVP level.

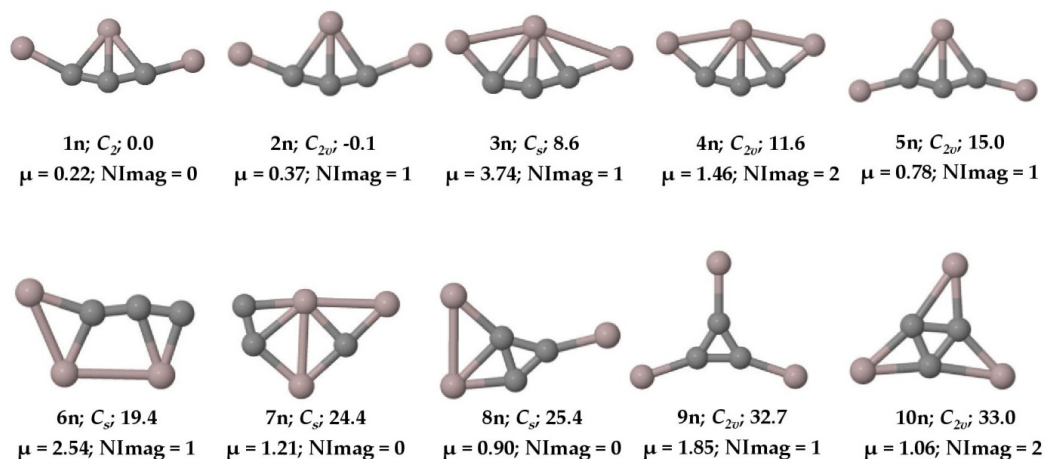


Figure 2. Ten low-lying isomers of Al_3C_3 with ZPVE-corrected relative energies (in kcal mol^{-1}), dipole moments (in Debye), and the number of imaginary frequencies (NImag) obtained at the PBE0-D3/def2-TZVP level.

Various aluminum–carbon clusters have continuously been investigated [16,17,49–52] as they have potential applications in energy storage [53] and the production of nano-powders [54,55] and solar cells [56]. Zheng and coworkers theoretically and experimentally explored the $\text{Al}_4\text{C}_6^{-/0}$ system and found that the global minimum isomer in the neutral state contains the planar hexa-coordinate aluminum [57]. In 2022, Kalita et al. reported the planar penta-coordinate Al and Ga centers in Cu_5Al_2^+ and Cu_5Ga_2^+ systems, which were global minimum structures, and found that the stabilizing factor was σ -aromaticity [58].

Recently, Malhan et al. reported the $\text{Al}_2\text{C}_4\text{H}_2$ system with ptC, planar tetra-coordinate aluminum (ptAl), and planar penta-coordinate aluminum (ppAl) atoms with aromatic characteristics [59]. The aforementioned discoveries have also inspired researchers to look for further systems containing hyper-coordinate main group elements, such as group 13 elements. Wang and coworkers reported B_8^- and B_9^- clusters exhibiting planar hepta- and octa-coordinate central boron atoms with combined experimental and computational studies [60]. Li et al. reported the global minimum structure of the BCu_5H_5^- system with planar penta-coordinate boron (ppB) [61]. The global minimum isomer containing the ppB atom in the B_6H_5^+ system with aromatic characteristics was reported by Wu and coworkers. In 2021, Khatun et al. reported $\text{BAI}_4\text{Mg}^{-/0/+}$ [62], in which the global minimum structures were found to have a planar tetra-coordinate boron (ptB) atom in its anionic and cationic forms as well as a ppB atom in the neutral state. In 2022, Das and coworkers explored the potential energy surface of $\text{CB}_6\text{Al}^{0/+}$ [63] and found that both neutral and cation contain planar hexa-coordinate boron (phB) atoms in their global minima. Thompson et al. experimentally reported the ptAl species [64]. The ptAl species of calix [4] pyrrole aluminate was also experimentally reported by Greb and coworkers in 2019 [65]. In 2023, Merino and coworkers also reported a quasi-ptC atom in the CAI_{11}^- system [66]. These distinctive bonding arrangements demonstrate not only the fundamental importance of improving our knowledge of chemical bonding but also a completely new class of molecules in the world of chemistry. Herein, the present work reports the $\text{Al}_3\text{C}_3^{-/0}$ system with tri-coordination; that is, five bonds to the central allenic carbon atom via computational quantum chemical modeling. The aluminum and carbon-based molecules have potential applications ranging from cluster assembled materials [67,68], energy storage [69], and two-dimensional donor materials in solar cells [70]. Dong et al. [71] have already reported the isomer **2n** of the Al_3C_3 system with hydrogen storage properties both experimentally and theoretically at MP2/6-311+G* level of theory, which gives us confidence that the $\text{Al}_3\text{C}_3^{-/0}$ system investigated here, has a high chance of synthetic viability in the future.

2. Computational Methodology

The initial geometries of the $\text{Al}_3\text{C}_3^{-/0}$ system were first generated through chemical intuition, and then, using the in-house Python code, all other possible geometries were explored on these two potential energy surfaces (PESs) using density functional theory (DFT). All geometries were fully optimized using the hybrid functional PBE0 [72] coupled with Grimme's dispersion correction (D3) [73,74] and the def2-TZVP [75,76] basis set. Frequency calculations were carried out at the same level of theory to ensure whether the optimized geometries are true minima or maxima or higher-order saddle points. To get more characteristic features on the chemical bonding of isomers **1a** and **1n**, the natural bond order (NBO) analysis [77], adaptive natural density partitioning (AdNDP) analysis [78,79], and Wiberg bond indices (WBIs) [80] were performed at the PBE0-D3/def2-TZVP level. The nucleus-independent chemical shift (NICS) [81] calculations for **1a** and **1n** structures were carried out at the same level to analyze the aromatic behavior of these systems. Atoms in molecules (AIM) analysis [82] of the Laplacian of electron density and electron localization function (ELF) [83] were carried out for isomers **1a** and **1n** using the wave function file generated by the Gaussian program [84] at the PBE0-D3/def2-TZVP level. The dynamic stabilities of **1a** and **1n** were evaluated using the atom-centered density matrix propagation (ADMP) [85] at the same level of theory. The AdNDP and ELF were analyzed through the Multiwfn program [86]. All the calculations were performed using the Gaussian 16 package [84].

3. Results and Discussion

The PESs of the $\text{Al}_3\text{C}_3^{-/0}$ are explored, and we found that the global minimum energy geometry (**1a** and **1n**) of both the anion and neutral system contains a carbon atom (C4) with two π bonds and three σ bonds, exhibiting a total of five bonds through tri-coordination. The ten low-lying isomers of the anion and the neutral system are given in

Figures 1 and 2, respectively. All other isomers on the PES of the $\text{Al}_3\text{C}_3^{-/0}$ system are given in the Supplementary Materials in Figures S1 and S2, respectively. The Al_3C_3^- system has a singlet spin state and the Al_3C_3 system corresponds to a doublet. Isomer **1a** is a planar structure with C_{2v} symmetry, whereas isomer **1n** shows C_2 symmetry, in which the terminal aluminum atoms are out of the plane (see Figure 3). The $\text{Al}_3\text{C}_3^{-/0}$ system also has structures that exhibit planar penta-coordinate aluminum (ppAl) and planar tetra-coordinate carbon (ptC) atoms as local minimum energy isomers (**8a**, **7n**; and **3a**, **13a**, and **8n**, respectively) on their PESs. Nevertheless, our focus here is on the global minimum energy isomers, **1a** and **1n**, which exhibit five bonds to carbon through tri-coordination.

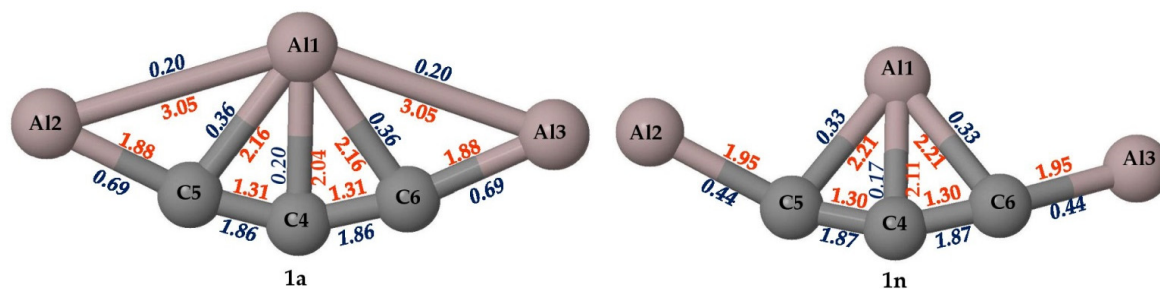


Figure 3. The bond lengths (in Å, red) and the Wiberg bond orders (in blue) are obtained at the PBE0-D3/def2-TZVP level for isomers **1a** and **1n**.

3.1. Wiberg Bond Indices

The WBI values obtained from NBO analysis for the allenic carbon (C4) atom in isomers **1a** and **1n** are critically analyzed. The WBI values and the bond distances are given in Figure 3. The standard covalent bond lengths of C–Al and C=C are 2.01 and 1.34 Å, respectively, which are in close agreement with the obtained values. The C4–Al1 bond length of isomer **1n** having 2.11 Å is slightly higher than that of isomer **1a** with 2.04 Å. The WBI values for the C=C bond in isomers **1a** and **1n** are 1.86 and 1.87, respectively, which confirms the presence of π bonds in both isomers. This further proves that in both cases, the C4 atom makes two π bonds with neighboring atoms. The C4–Al1 bond with WBI values of 0.20 and 0.17 in isomers **1a** and **1n** suggests the dative bonding nature of the fifth bond. The total bond order of C4 in isomers **1a** and **1n** is 3.99 and 3.97, respectively. This indicates that the allenic carbon atom, C4, is surrounded by eight electrons but still makes two π bonds with neighboring carbon atoms and also forms an additional dative bond with the central aluminum atom.

3.2. Adaptive Natural Density Partitioning (AdNDP) Analysis

To further analyze the bonding scenario, the AdNDP analysis was carried out for the delineation of n -center 2-electron (nc -2e) bonds in the investigated systems. The generated AdNDP orbitals with occupation numbers (ON) for isomers **1a** and **1n** are shown in Figure 4. As the neutral system is in a doublet state, only alpha orbitals are considered for this analysis. The tri-coordinated C4 atom has two $2c$ -2e σ and two $2c$ -2e π bonds with its neighboring carbon atoms, with ON 1.99 $|e|$ and 1.85 $|e|$, respectively, which confirms the presence of alternating π bonds in the isomer **1a**. It also exhibits delocalization of electron densities through $3c$ -2e σ , $4c$ -2e σ , $3c$ -2e π , and $4c$ -2e π bonds with ON ranging from 1.89 $|e|$ to 2.00 $|e|$, which support the tri-coordination in the structure. The two $2c$ -2e π bonds in isomer **1n** confirm the presence of alternating π bonds which also exhibit delocalization of electron densities through multi-center 2e σ and π bonds, which supports the structural stability. To support the observed AdNDP bonding pattern, the nucleus-independent chemical shift (NICS) values are also calculated for isomers **1a** and **1n**, which are shown in Figure S3. The negative values of NICS (0) and NICS (1) also confirm the presence σ - and π -aromatic nature in both the isomers, respectively.

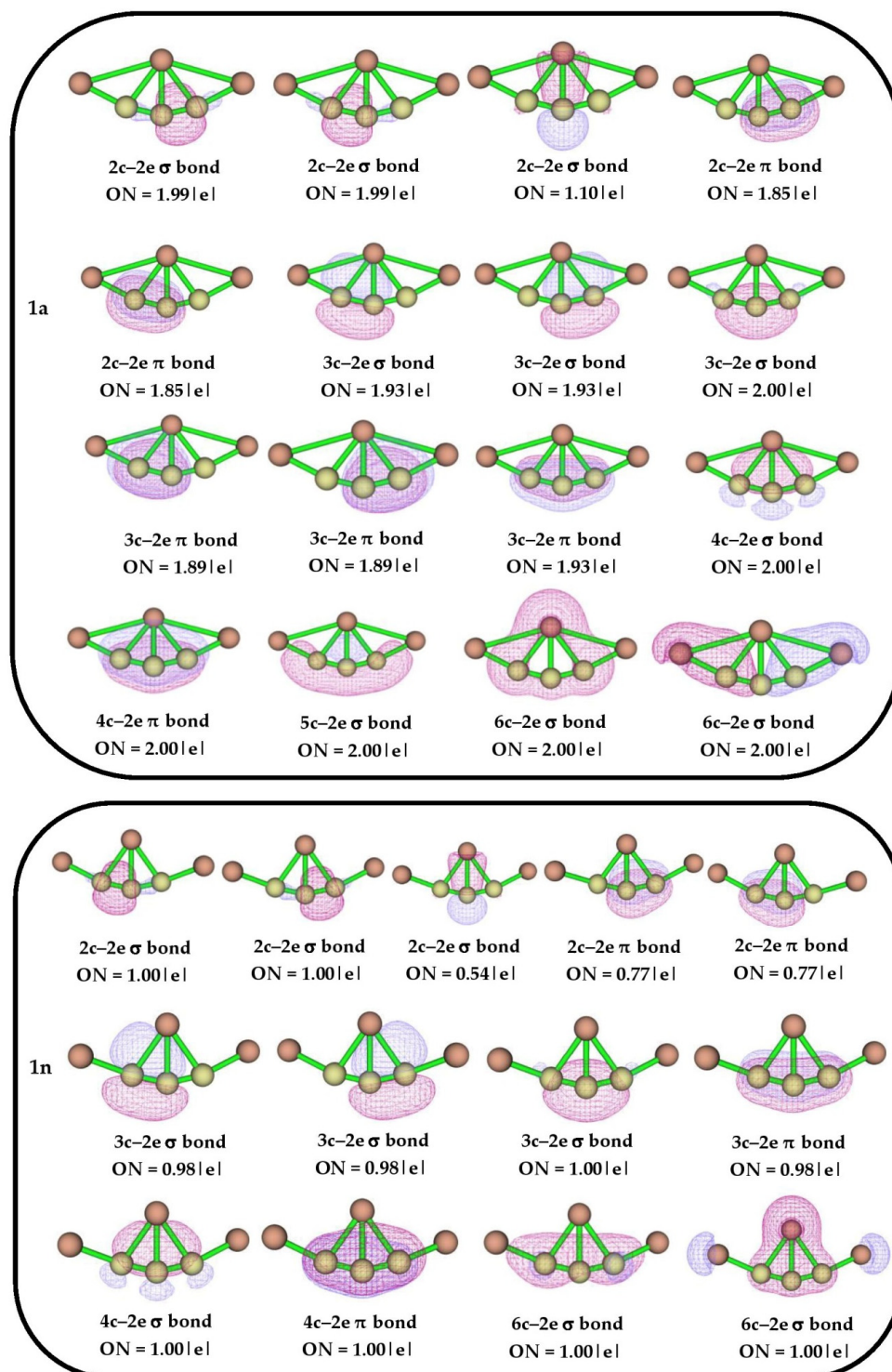


Figure 4. AdNDP bonding patterns with occupation numbers (ONs) for isomers **1a** and **1n**.

3.3. Atoms in Molecule (AIM) Analysis

The AIM analysis is carried out to gain insight into the bonding characteristic features. The color-filled plots of the electron localization function (ELF) and contour diagram for the Laplacian of electron density ($\Delta^2\rho(r)$) for isomers **1a** and **1n** are shown in Figure 5. The ELF plot of isomers **1a** indicates the interaction of the C4 atom with its neighboring atoms and supports the delocalization of electron densities within the molecule. Apart from the terminal Al2 and Al3 atoms, which are out of the plane, isomer **1n** also supports the delocalization of electron densities around the C4 atom. In **1a**, bond critical points (BCPs)

between the C4 and its neighboring atoms support the existence of bond paths. Isomer **1n** has BCPs between C4 and its adjacent carbon atoms and also has a ring critical point (RCP) which dictates the dominant aromatic characteristics in the structure.

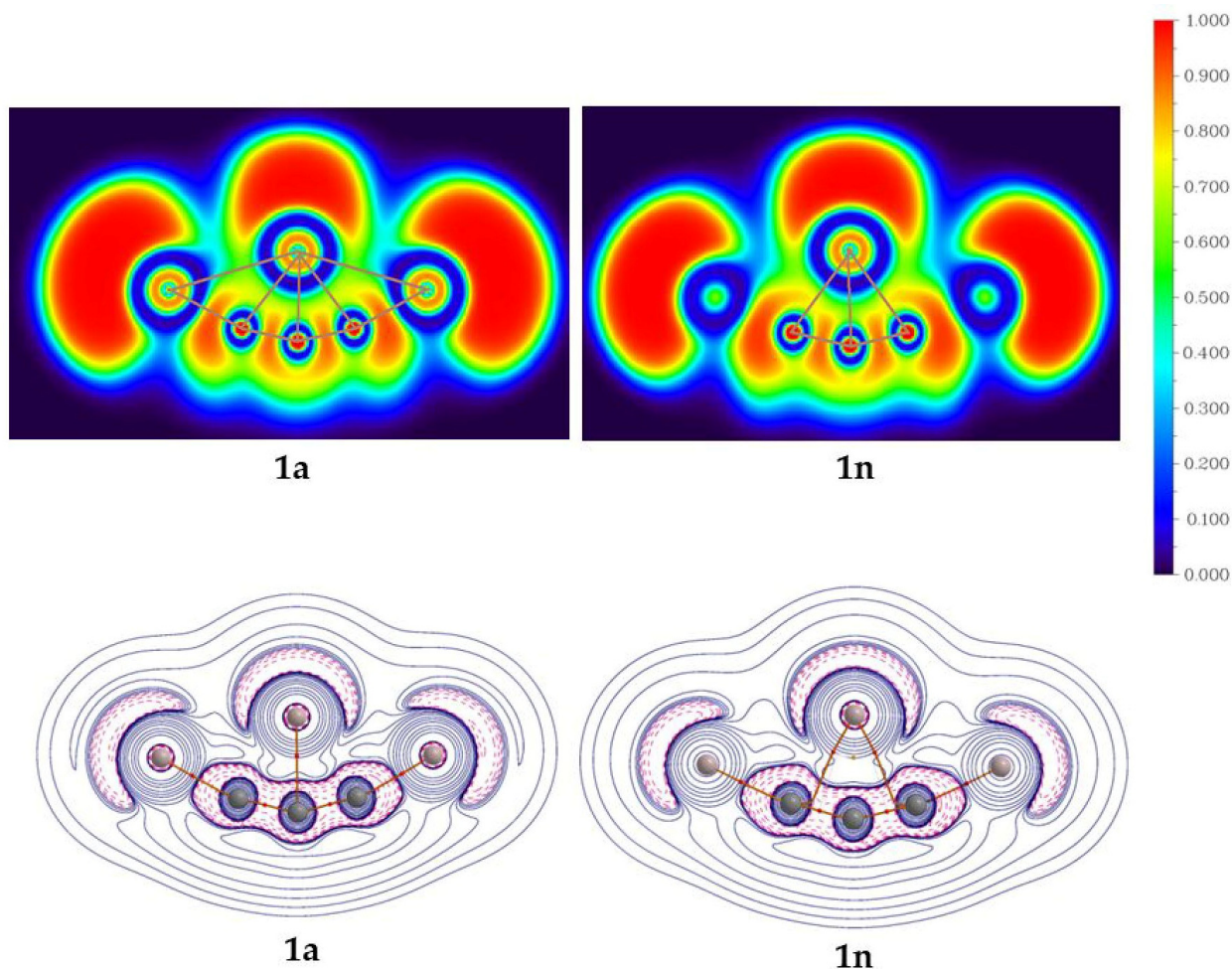


Figure 5. The color-filled map of ELF (top row) and the Laplacian of electron density ($\Delta^2\rho(r)$) with bond paths (bottom row) for isomers **1a** and **1n** at the PBE0-D3/def2-TZVP level.

3.4. Kinetic Stability

The ab initio molecular dynamics (AIMD) simulations are carried out for 3000 fs at 298 K and 1 atm pressure using the ADMP approach to explore the kinetic stability of the investigated structures. The time evolution of energy plots for isomers **1a** and **1n** are given in Figure 6. Slight structural deformation occurs during the simulation, which causes an increase in nuclear kinetic energy. However, the present data reveal that the overall geometry is not completely destroyed, which indicates that these molecules are kinetically stable apart from their thermodynamic stability. As expected, for both isomers **1a** and **1n**, the five bonds to the C4 atom remain the same throughout the simulation period. The structural stability of these isomers is well maintained during the simulation, and no isomerization or other structural modifications occur in these molecules, suggesting that they are indeed kinetically stable.

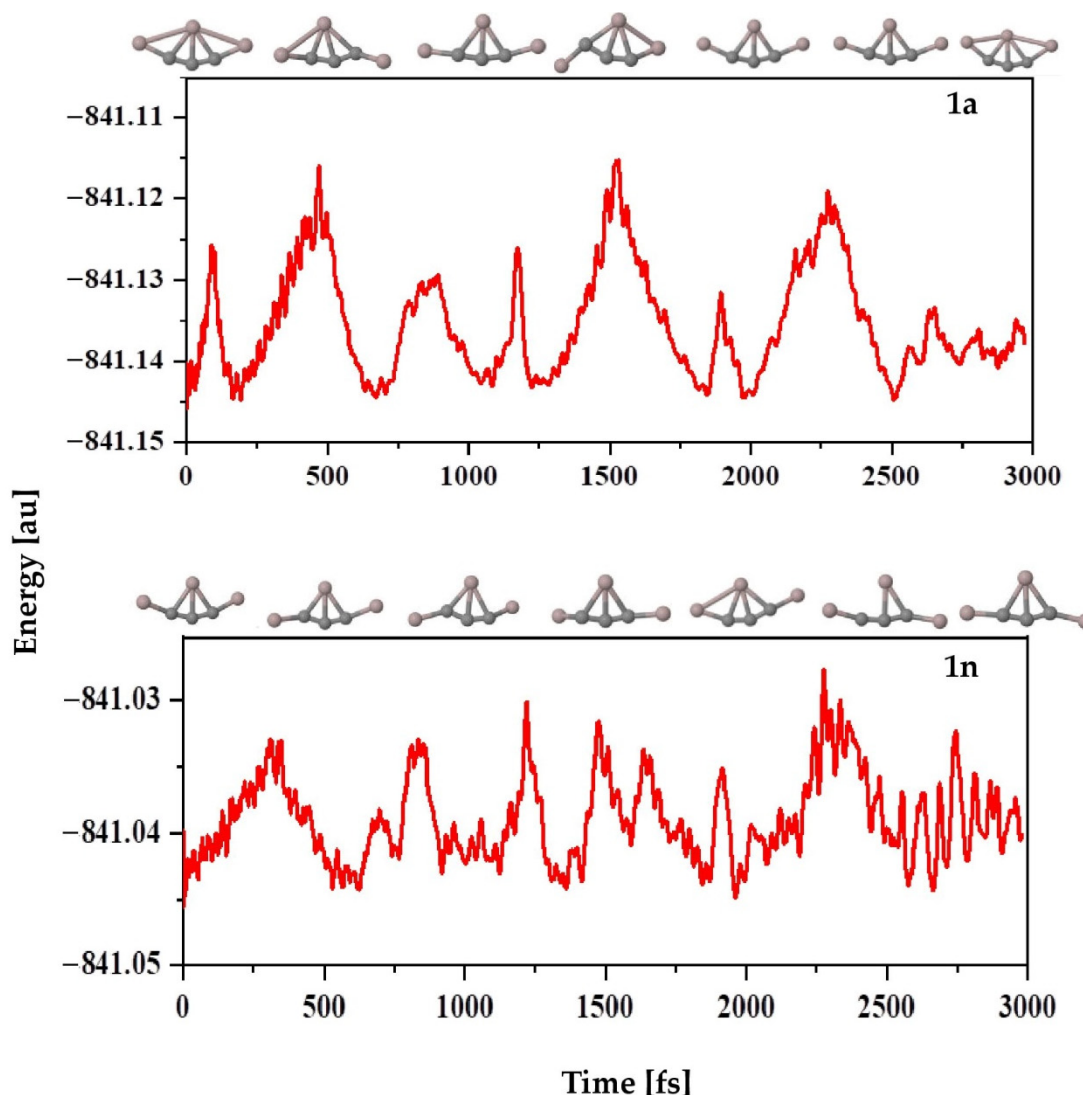


Figure 6. Time evolution of the total energy of isomers **1a** (top) and **1n** (bottom) calculated at the PBE0-D3/def2-TZVP level.

4. Conclusions

Using density functional theory, various isomers of the $\text{Al}_3\text{C}_3^{-/0}$ system were explored first by chemical intuition, and other possible isomers are then identified with the help of the in-house Python code. The global minimum isomers **1a** and **1n** exhibit five bonds to carbon through tri-coordination. The present work reports for the first time five bonds to carbon through tri-coordination in the $\text{Al}_3\text{C}_3^{-/0}$ system as observed in isomers **1a** and **1n**, respectively. Isomer **1a** is a planar structure with C_{2v} symmetry, whereas isomer **1n** shows C_2 symmetry with the terminal aluminum atoms out of the plane. WBI analysis indicates that the central allenic carbon atom in both the isomers (**1a** and **1n**) forms five bonds through tri-coordination and also obeys the octet rule simultaneously. The BCPs from AIM analysis confirm the presence of bond paths between allenic carbon and its adjacent atoms. The aromatic nature that stabilizes both the isomers **1a** and **1n** is well supported by AdNDP, ELF, and NICS analyses. Both the isomers are kinetically stable as inferred from the ab initio molecular dynamics simulations at 1 atm pressure and 298 K temperature up to 3000 fs of time. The obtained results on the $\text{Al}_3\text{C}_3^{-/0}$ system via computational calculations may encourage experimentalists to design this new class of molecules in the future.

Supplementary Materials: The following supporting information can be downloaded at: <https://www.mdpi.com/article/10.3390/chemistry5020076/s1>, The optimized geometries of all Al_3C_3^- and Al_3C_3 isomers are given in Figures S1 and S2, respectively, NICSs in ppm for the isomers **1a** and **1n** are given in Figure S3, AdNDP bonding patterns with occupation numbers (ONs) for isomers **1a** and **1n** are given in Figures S4 and S5, respectively, total energies (in a.u), Zero-point vibrational energies (ZPVEs; in a.u), ZPVE corrected total energies (E+ZPVE; in a.u), relative energies (ΔE +ZPVE; in kcal mol⁻¹), and the number of imaginary frequencies (NImag) of all Al_3C_3^- and Al_3C_3 isomers at PBE0-D3/def2-TZVP level are given in Tables S1 and S2, respectively, and Cartesian coordinates of all Al_3C_3^- and Al_3C_3 isomers at the PBE0-D3/def2-TZVP level are given in Tables S3 and S4, respectively.

Author Contributions: Conceptualization, V.S.T. and K.T.; Investigation, A.H.M., V.S.T. and K.T.; Methodology, A.H.M., V.S.T. and K.T.; Supervision, V.S.T. and K.T.; Visualization, A.H.M. and K.T.; Writing—original draft, A.H.M. and V.S.T.; Writing—review and editing, V.S.T. and K.T. All authors have read and agreed to the published version of the manuscript.

Funding: This research received no external funding.

Institutional Review Board Statement: Not applicable.

Informed Consent Statement: Not applicable.

Data Availability Statement: Data are available in the article or Supplementary Materials.

Acknowledgments: The computational facility provided at the VIT, Vellore, to carry out this work is gratefully acknowledged.

Conflicts of Interest: The authors declare no conflict of interest.

References

1. Tal'rose, V.L.; Lyubimova, A.K. Secondary Processes in the Ion Source of the Mass Spectrometer. *Dokl. Akad. Nauk SSSR* **1952**, *86*, 909–912.
2. White, E.T.; Tang, J.; Oka, T. CH_5^+ : The Infrared Spectrum Observed. *Science* **1999**, *284*, 135–137. [[CrossRef](#)]
3. Schleyer, P.v.R.; Wuerthwein, E.U.; Kaufmann, E.; Clark, T.; Pople, J.A. Effectively Hypervalent Molecules. 2. Lithium Carbide (CLi_5), Lithium Carbide (CLi_6), and the Related Effectively Hypervalent First Row Molecules, $\text{CLi}_5\text{-NH}_n$ and $\text{CLi}_6\text{-NH}_n$. *J. Am. Chem. Soc.* **1983**, *105*, 5930–5932. [[CrossRef](#)]
4. Kudo, H. Observation of Hypervalent CLi_6 by Knudsen-Effusion Mass Spectrometry. *Nature* **1992**, *355*, 432–434. [[CrossRef](#)]
5. Dávalos, J.Z.; Herrero, R.; Abboud, J.-L.M.; Mó, O.; Yáñez, M. How can a Carbon Atom Be Covalently Bound to Five Ligands? The Case of $\text{Si}_2(\text{CH}_3)_7^+$. *Angew. Chem. Int. Ed.* **2006**, *46*, 381–385. [[CrossRef](#)]
6. McKee, W.C.; Agarwal, J.; Schaefer, H.F.; Schleyer, P.V.R. Covalent Hypercoordination: Can Carbon Bind Five Methyl Ligands? *Angew. Chem. Int. Ed.* **2014**, *53*, 7875–7878. [[CrossRef](#)]
7. Hogeveen, H.; Kwant, P.W. Direct observation of a remarkably stable dication of unusual structure: $(\text{CCH}_3)_6^{2+}$. *Tetrahedron Lett.* **1973**, *14*, 1665–1670. [[CrossRef](#)]
8. Schmidbaur, H.; Gabbaie, F.; Schier, A.; Riede, J. Hypercoordinate Carbon in Protonated Tetraauriomethane Molecules. *Organometallics* **1995**, *14*, 4969–4971. [[CrossRef](#)]
9. Scherbaum, F.; Grohmann, A.; Müller, G.; Schmidbaur, H. Synthesis, Structure, and Bonding of the Cation $[(\text{C}_6\text{H}_5)_3\text{PAu}_5\text{C}]^+$. *Angew. Chem. Int. Ed.* **1989**, *28*, 463–465. [[CrossRef](#)]
10. Scherbaum, F.; Grohmann, A.; Huber, B.; Krüger, C.; Schmidbaur, H. "Aurophilicity" as a Consequence of Relativistic Effects: The Hexakis (Triphenylphosphaneaurio) Methane Dication $[(\text{Ph}_3\text{PAu})_6\text{C}]^{2+}$. *Angew. Chem. Int. Ed.* **1988**, *27*, 1544–1546. [[CrossRef](#)]
11. Malischewski, M.; Seppelt, K. Crystal Structure Determination of the Pentagonal-Pyramidal Hexamethylbenzene Dication $\text{C}_6(\text{CH}_3)_6^{2+}$. *Angew. Chem. Int. Ed.* **2017**, *56*, 368–370. [[CrossRef](#)]
12. Akiba, K.; Yamashita, M.; Yamamoto, Y.; Nagase, S. Synthesis and Isolation of Stable Hypervalent Carbon Compound (10-C-5) Bearing a 1,8-Dimethoxyanthracene Ligand. *J. Am. Chem. Soc.* **1999**, *121*, 10644–10645. [[CrossRef](#)]
13. Yamaguchi, T.; Yamamoto, Y.; Kinoshita, D.; Akiba, K.; Zhang, Y.; Reed, C.A.; Hashizume, D.; Iwasaki, F. Synthesis and Structure of a Hexacoordinate Carbon Compound. *J. Am. Chem. Soc.* **2008**, *130*, 6894–6895. [[CrossRef](#)]
14. Lancaster, K.M.; Roemelt, M.; Ettenhuber, P.; Hu, Y.; Ribbe, M.W.; Neese, F.; Bergmann, U.; DeBeer, S. X-Ray Emission Spectroscopy Evidences a Central Carbon in the Nitrogenase Iron-Molybdenum Cofactor. *Science* **2011**, *334*, 974–977. [[CrossRef](#)]
15. Hoffmann, R.; Alder, R.W.; Wilcox, C.F. Planar Tetracoordinate Carbon. *J. Am. Chem. Soc.* **1970**, *92*, 4992–4993. [[CrossRef](#)]
16. Li, X.; Wang, L.-S.; Boldyrev, A.I.; Simons, J. Tetracoordinated Planar Carbon in the Al_4C^- Anion. A Combined Photoelectron Spectroscopy and Ab Initio Study. *J. Am. Chem. Soc.* **1999**, *121*, 6033–6038. [[CrossRef](#)]
17. Li, X.; Zhang, H.-F.; Wang, L.-S.; Geske, G.D.; Boldyrev, A.I. Pentaatomic Tetracoordinate Planar Carbon, $[\text{CA}_4]^{2-}$: A New Structural Unit and Its Salt Complexes. *Angew. Chem.* **2000**, *39*, 3630–3632. [[CrossRef](#)]

18. Keese, R. Carbon Flatland: Planar Tetracoordinate Carbon and Fenestranes. *Chem. Rev.* **2006**, *106*, 4787–4808. [[CrossRef](#)]
19. Xu, J.; Zhang, X.; Yu, S.; Ding, Y.; Bowen, K.H. Identifying the Hydrogenated Planar Tetracoordinate Carbon: A Combined Experimental and Theoretical Study of CA_4H and CA_4H^- . *J. Phys. Chem. Lett.* **2017**, *8*, 2263–2267. [[CrossRef](#)] [[PubMed](#)]
20. Jia, X.; Du, Z. 18-Valence-Electron Rule Lighted Planar Tetracoordinate Carbon and Nitrogen: The Global Energy Minima of CA_4Zn and NA_4Zn^+ . *Phys. Chem. Chem. Phys.* **2023**, *25*, 4211–4215. [[CrossRef](#)] [[PubMed](#)]
21. Das, P.; Khatun, M.; Anoop, A.; Chattaraj, P.K. $CSi_nGe_{4-n}^{2+}$ ($n = 1-3$): Prospective Systems Containing Planar Tetracoordinate Carbon (PtC). *Phys. Chem. Chem. Phys.* **2022**, *24*, 16701–16711. [[CrossRef](#)] [[PubMed](#)]
22. Das, P.; Chattaraj, P.K. $CSiGaAl_2^{-/0}$ and $CGeGaAl_2^{-/0}$ Having Planar Tetracoordinate Carbon Atoms in Their Global Minimum Energy Structures. *J. Comput. Chem.* **2022**, *43*, 894–905. [[CrossRef](#)] [[PubMed](#)]
23. Leyva-Parra, L.; Inostroza, D.; Yañez, O.; Cruz, J.C.; Garza, J.; García, V.; Tiznado, W. Persistent Planar Tetracoordinate Carbon in Global Minima Structures of Silicon-Carbon Clusters. *Atoms* **2022**, *10*, 27. [[CrossRef](#)]
24. Liu, F.-L.; Guo, J.-C. Ternary CE_2Ba_2 ($E = As, Sb$) Clusters: New Pentaatomic Planar Tetracoordinate Carbon Species with 18 Valence Electrons. *J. Mol. Model.* **2022**, *28*, 230. [[CrossRef](#)]
25. Thirumoorthy, K.; Chandrasekaran, V.; Cooksy, A.L.; Thimmakondur, V.S. Kinetic Stability of $Si_2C_5H_2$ Isomer with a Planar Tetracoordinate Carbon Atom. *Chemistry* **2020**, *3*, 13–27. [[CrossRef](#)]
26. Thirumoorthy, K.; Karton, A.; Thimmakondur, V.S. From High-Energy C_7H_2 Isomers with a Planar Tetracoordinate Carbon Atom to an Experimentally Known Carbene. *J. Phys. Chem. A* **2018**, *122*, 9054–9064. [[CrossRef](#)] [[PubMed](#)]
27. Thimmakondur, V.S.; Thirumoorthy, K. $Si_3C_2H_2$ Isomers with a Planar Tetracoordinate Carbon or Silicon Atom(s). *Comput. Theor. Chem.* **2019**, *1157*, 40–46. [[CrossRef](#)]
28. Jayakumari, C.; Nag, P.; Isukapalli, S.; Vennapusa, S. Exploring the Excited-State Nonadiabatic Effects in the Semisaturated Planar Tetracoordinated Carbon Molecule C_7H_4 . *Atoms* **2022**, *10*, 10. [[CrossRef](#)]
29. Job, N.; Khatun, M.; Thirumoorthy, K.; CH, S.S.R.; Chandrasekaran, V.; Anoop, A.; Thimmakondur, V.S. $CA_4Mg^{0/-}$: Global Minima with a Planar Tetracoordinate Carbon Atom. *Atoms* **2021**, *9*, 24. [[CrossRef](#)]
30. Thirumoorthy, K.; Thimmakondur, V.S. Flat Crown Ethers with Planar Tetracoordinate Carbon Atoms. *Int. J. Quantum Chem.* **2021**, *121*, e26479. [[CrossRef](#)]
31. Pei, Y.; An, W.; Ito, K.; Schleyer, P.V.R.; Xiao, C.Z. Planar Pentacoordinate Carbon in CA_5^+ : A Global Minimum. *J. Am. Chem. Soc.* **2008**, *130*, 10394–10400. [[CrossRef](#)] [[PubMed](#)]
32. Jimenez-Halla, J.O.C.; Wu, Y.-B.; Wang, Z.-X.; Islas, R.; Heine, T.; Merino, G. CA_4Be and CA_3Be^{2-} : Global Minima with a Planar Pentacoordinate Carbon Atom. *Chem. Commun.* **2010**, *46*, 8776. [[CrossRef](#)] [[PubMed](#)]
33. Pan, S.; Cabellos, J.L.; Orozco-Ic, M.; Chattaraj, P.K.; Zhao, L.; Merino, G. Planar Pentacoordinate Carbon in CGa_5^+ Derivatives. *Phys. Chem. Chem. Phys.* **2018**, *20*, 12350–12355. [[CrossRef](#)]
34. Das, P.; Chattaraj, P.K. Structure and Bonding in Planar Hypercoordinate Carbon Compounds. *Chemistry* **2022**, *4*, 1723–1756. [[CrossRef](#)]
35. Sarkar, P.; Thirumoorthy, K.; Anoop, A.; Thimmakondur, V.S. Planar Pentacoordinate Carbon in $[XC_7H_2]^{2+}$ ($X = Be$ and Mg) and Its Derivatives. *Phys. Chem. Chem. Phys.* **2022**, *24*, 27606–27611. [[CrossRef](#)] [[PubMed](#)]
36. Sun, R.; Jin, B.; Huo, B.; Yuan, C.; Zhai, H.-J.; Wu, Y.-B. Planar Pentacoordinate Carbon in a Sulphur-Surrounded Boron Wheel: The Global Minimum of $CB_5S_5^+$. *Chem. Commun.* **2022**, *58*, 2552–2555. [[CrossRef](#)]
37. Sun, R.; Zhao, X.-F.; Jin, B.; Huo, B.; Bian, J.-H.; Guan, X.-L.; Yuan, C.; Wu, Y.-B. Influence of Stepwise Oxidation on the Structure, Stability, and Properties of Planar Pentacoordinate Carbon Species CA_5^+ . *Phys. Chem. Chem. Phys.* **2020**, *22*, 17062–17067. [[CrossRef](#)]
38. Das, P.; Pan, S.; Chattaraj, P.K. Planar Hypercoordinate Carbon. In *Atomic Clusters with Unusual Structure, Bonding and Reactivity*; Elsevier: Amsterdam, The Netherlands, 2023; pp. 357–372.
39. Vassilev-Galindo, V.; Pan, S.; Donald, K.J.; Merino, G. Planar Pentacoordinate Carbons. *Nat. Rev. Chem.* **2018**, *2*, 0114. [[CrossRef](#)]
40. Yang, L.-M.; Ganz, E.; Chen, Z.; Wang, Z.-X.; Schleyer, P.V.R. Four Decades of the Chemistry of Planar Hypercoordinate Compounds. *Angew. Chem. Int. Ed.* **2015**, *54*, 9468–9501. [[CrossRef](#)]
41. Exner, K.; Schleyer, P.V.R. Planar Hexacoordinate Carbon: A Viable Possibility. *Science* **2000**, *290*, 1937–1940. [[CrossRef](#)]
42. Ito, K.; Chen, Z.F.; Corminboeuf, C.; Wannere, C.S.; Zhang, X.H.; Li, Q.S.; Schleyer, P.V.R. Myriad Planar Hexacoordinate Carbon Molecules Inviting Synthesis. *J. Am. Chem. Soc.* **2007**, *129*, 1510–1511. [[CrossRef](#)]
43. Inostroza, D.; Leyva-Parra, L.; Yañez, O.; Solar-Encinas, J.; Vásquez-Espinal, A.; Valenzuela, M.L.; Tiznado, W. Searching for Systems with Planar Hexacoordinate Carbons. *Atoms* **2023**, *11*, 56. [[CrossRef](#)]
44. Leyva-Parra, L.; Diego, L.; Yañez, O.; Inostroza, D.; Barroso, J.; Vásquez-Espinal, A.; Merino, G.; Tiznado, W. Planar Hexacoordinate Carbons: Half Covalent, Half Ionic. *Angew. Chem. Int. Ed.* **2021**, *60*, 8700–8704. [[CrossRef](#)] [[PubMed](#)]
45. Bradley, J.S.; Ansell, G.B.; Leonowicz, M.E.; Hill, E.W. Synthesis and Molecular Structure of μ_4 -Carbido- μ_2 -Carbonyl-Dodecacarbonyltetrairon, a Neutral Iron Butterfly Cluster Bearing an Exposed Carbon Atom. *J. Am. Chem. Soc.* **1981**, *103*, 4968–4970. [[CrossRef](#)]
46. Radius, U.; Silverio, S.J.; Hoffmann, R.; Gleiter, R. A Five-Coordinate Carbon Center and Zr to H, B, and C Bonding in $Cp_2Zr[CH_2(BH(C_6F_5)_2)_2]$. *Organometallics* **1996**, *15*, 3737–3745. [[CrossRef](#)]
47. Vicente, J.; Chicote, M.T.; Guerrero, R.; Jones, P.G. Synthesis of the First Complex with a Hypercoordinate Ylidic Carbon Atom. Crystal and Molecular Structure of $[Au(PPh_3)_4CS(=O)Me_2](ClO_4)_2$. *J. Am. Chem. Soc.* **1996**, *118*, 699–700. [[CrossRef](#)]

48. Shajan, S.; Guo, J.-C.; Sinjari, A.; Thirumoorthy, K.; Thimmakonda, V.S. Pentacoordinate Carbon Atoms in a Ferrocene Dication Derivative— $[\text{Fe}(\text{Si}_2\text{-H}_5\text{-C}_5\text{H}_2)_2]^{2+}$. *Chemistry* **2022**, *4*, 1092–1100. [[CrossRef](#)]
49. Zhang, C.-J.; Wang, P.; Xu, X.-L.; Xu, H.-G.; Zheng, W.-J. Photoelectron Spectroscopy and Theoretical Study of $\text{Al}_n\text{C}_5^{-/0}$ ($n = 1\text{--}5$) Clusters: Structural Evolution, Relative Stability of Star-like Clusters, and Planar Tetracoordinate Carbon Structures. *Phys. Chem. Chem. Phys.* **2021**, *23*, 1967–1975. [[CrossRef](#)] [[PubMed](#)]
50. Ravell, E.; Jalife, S.; Barroso, J.; Orozco-Ic, M.; Hernández-Juárez, G.; Ortiz-Chi, F.; Pan, S.; Cabellos, J.L.; Merino, G. Structure and Bonding in CE_5^- ($\text{E} = \text{Al-Tl}$) Clusters: Planar Tetracoordinate Carbon versus Pentacoordinate Carbon. *Chem. Asian J.* **2018**, *13*, 1467–1473. [[CrossRef](#)]
51. Wu, Y.; Jiang, J.; Lu, H.; Wang, Z.; Perez-Peralta, N.; Islas, R.; Contreras, M.; Merino, G.; Wu, J.I.; von Ragué Schleyer, P. Starlike Aluminum–Carbon Aromatic Species. *Chem. A Eur. J.* **2011**, *17*, 714–719. [[CrossRef](#)]
52. Bai, L.-X.; Guo, J.-C. CA_4X_4 ($\text{X} = \text{Te, Po}$): Double Aromatic Molecular Stars Containing Planar Tetracoordinate Carbon Atoms. *Molecules* **2023**, *28*, 3280. [[CrossRef](#)] [[PubMed](#)]
53. Yang, H.; Zhang, Y.; Chen, H. Dissociation of H_2 on Carbon Doped Aluminum Cluster Al_6C . *J. Chem. Phys.* **2014**, *141*, 064302. [[CrossRef](#)] [[PubMed](#)]
54. Ermoline, A.; Schoenitz, M.; Dreizin, E.; Yao, N. Production of Carbon-Coated Aluminium Nanopowders in Pulsed Microarc Discharge. *Nanotechnology* **2002**, *13*, 638–643. [[CrossRef](#)]
55. Kotov, Y.A.; Beketov, I.V.; Medvedev, A.I.; Murzakaev, A.M.; Timoshenkova, O.P.; Demina, T.M. Forming a Carbide Coating on the Surface of Aluminum Nanoparticles and Producing Nanopowders from $\text{Al-Al}_4\text{C}_3$ Using the Method of Electric Explosion of Wire. *Nanotechnol. Russ.* **2010**, *5*, 831–836. [[CrossRef](#)]
56. Li, Y.; Liao, Y.; Schleyer, P.v.R.; Chen, Z. Al_2C Monolayer: The Planar Tetracoordinate Carbon Global Minimum. *Nanoscale* **2014**, *6*, 10784. [[CrossRef](#)]
57. Zhang, C.-J.; Xu, H.-G.; Xu, X.-L.; Zheng, W.-J. Anion Photoelectron Spectroscopy and Theoretical Studies of $\text{Al}_4\text{C}_6^{-/0}$: Global Minimum Triangle-Shaped Structures and Hexacoordinated Aluminum. *J. Phys. Chem. A* **2021**, *125*, 302–307. [[CrossRef](#)]
58. Kalita, A.J.; Sarmah, K.; Yashmin, F.; Borah, R.R.; Baruah, I.; Deka, R.P.; Guha, A.K. σ -Aromaticity in Planar Pentacoordinate Aluminium and Gallium Clusters. *Sci. Rep.* **2022**, *12*, 10041. [[CrossRef](#)]
59. Malhan, A.H.; Sobinson, S.; Job, N.; Shajan, S.; Mohanty, S.P.; Thimmakonda, V.S.; Thirumoorthy, K. $\text{Al}_2\text{C}_4\text{H}_2$ Isomers with the Planar Tetracoordinate Carbon (PtC)/Aluminum (PtAl). *Atoms* **2022**, *10*, 112. [[CrossRef](#)]
60. Zhai, H.-J.; Alexandrova, A.N.; Birch, K.A.; Boldyrev, A.I.; Wang, L.-S. Hepta- and Octacoordinate Boron in Molecular Wheels of Eight- and Nine-Atom Boron Clusters: Observation and Confirmation. *Angew. Chem.* **2003**, *115*, 6186–6190. [[CrossRef](#)]
61. Li, S.D.; Miao, C.Q.; Ren, G.M. D_{5h} $\text{Cu}_5\text{H}_5\text{X}$: Pentagonal Hydrocopper Cu_5H_5 Containing Pentacoordinate Planar Nonmetal Centers ($\text{X} = \text{B, C, N, O}$). *Eur. J. Inorg. Chem.* **2004**, 2232–2234. [[CrossRef](#)]
62. Khatun, M.; Roy, S.; Giri, S.; CH, S.S.R.; Anoop, A.; Thimmakonda, V.S. $\text{BA}_4\text{Mg}^{-/0/+}$: Global Minima with a Planar Tetracoordinate or Hypercoordinate Boron Atom. *Atoms* **2021**, *9*, 89. [[CrossRef](#)]
63. Das, P.; Patra, S.G.; Chattaraj, P.K. $\text{CB}_6\text{Al}^{0/+}$: Planar Hexacoordinate Boron (PhB) in the Global Minimum Structure. *Phys. Chem. Chem. Phys.* **2022**, *24*, 22634–22644. [[CrossRef](#)]
64. Thompson, E.J.; Myers, T.W.; Berben, L.A. Synthesis of Square-Planar Aluminum(III) Complexes. *Angew. Chem. Int. Ed.* **2014**, *53*, 14132–14134. [[CrossRef](#)]
65. Ebner, F.; Wadepohl, H.; Greb, L. Calix [4]Pyrrole Aluminate: A Planar Tetracoordinate Aluminum(III) Anion and Its Unusual Lewis Acidity. *J. Am. Chem. Soc.* **2019**, *141*, 18009–18012. [[CrossRef](#)]
66. Bai, L.-X.; Barroso, J.; Orozco-Ic, M.; Ortiz-Chi, F.; Guo, J.-C.; Merino, G. CA_{11}^- : A Molecular Rotor with a Quasi-Planar Tetracoordinate Carbon. *Chem. Commun.* **2023**, *59*, 4966–4969. [[CrossRef](#)] [[PubMed](#)]
67. Leskiw, B.D.; Castleman, A.W. The Interplay between the Electronic Structure and Reactivity of Aluminum Clusters: Model Systems as Building Blocks for Cluster Assembled Materials. *Chem. Phys. Lett.* **2000**, *316*, 31–36. [[CrossRef](#)]
68. Zhao, J.; Liu, B.; Zhai, H.; Zhou, R.; Ni, G.; Xu, Z. Mass Spectrometric and First Principles Study of Al_nC^- Clusters. *Solid State Commun.* **2002**, *122*, 543–547. [[CrossRef](#)]
69. Maatallah, M.; Guo, M.; Cherqaoui, D.; Jarid, A.; Liebman, J.F. Aluminium Clusters for Molecular Hydrogen Storage and the Corresponding Alanes as Fuel Alternatives: A Structural and Energetic Analysis. *Int. J. Hydrogen Energy* **2013**, *38*, 5758–5767. [[CrossRef](#)]
70. Dai, J.; Wu, X.; Yang, J.; Zeng, X.C. Al_xC Monolayer Sheets: Two-Dimensional Networks with Planar Tetracoordinate Carbon and Potential Applications as Donor Materials in Solar Cell. *J. Phys. Chem. Lett.* **2014**, *5*, 2058–2065. [[CrossRef](#)]
71. Dong, F.; Heinbuch, S.; Xie, Y.; Rocca, J.J.; Bernstein, E.R. Experimental and Theoretical Study of Neutral Al_mC_n and $\text{Al}_m\text{C}_n\text{H}_x$ Clusters. *Phys. Chem. Chem. Phys.* **2010**, *12*, 2569. [[CrossRef](#)]
72. Ernzerhof, M.; Perdew, J.P. Generalized Gradient Approximation to the Angle- and System-Averaged Exchange Hole. *J. Chem. Phys.* **1998**, *109*, 3313–3320. [[CrossRef](#)]
73. Adamo, C.; Barone, V. Toward Reliable Density Functional Methods without Adjustable Parameters: The PBE0 Model. *J. Chem. Phys.* **1999**, *110*, 6158–6170. [[CrossRef](#)]
74. Grimme, S.; Antony, J.; Ehrlich, S.; Krieg, H. A Consistent and Accurate Ab Initio Parametrization of Density Functional Dispersion Correction (DFT-D) for the 94 Elements H-Pu. *J. Chem. Phys.* **2010**, *132*, 154104. [[CrossRef](#)] [[PubMed](#)]

75. Weigend, F.; Ahlrichs, R. Balanced Basis Sets of Split Valence, Triple Zeta Valence and Quadruple Zeta Valence Quality for H to Rn: Design and Assessment of Accuracy. *Phys. Chem. Chem. Phys.* **2005**, *7*, 3297. [[CrossRef](#)]
76. Weigend, F. Accurate Coulomb-Fitting Basis Sets for H to Rn. *Phys. Chem. Chem. Phys.* **2006**, *8*, 1057. [[CrossRef](#)]
77. Reed, A.E.; Weinstock, R.B.; Weinhold, F. Natural Population Analysis. *J. Chem. Phys.* **1985**, *83*, 735–746. [[CrossRef](#)]
78. Zubarev, D.Y.; Boldyrev, A.I. Developing Paradigms of Chemical Bonding: Adaptive Natural Density Partitioning. *Phys. Chem. Chem. Phys.* **2008**, *10*, 5207. [[CrossRef](#)]
79. Zubarev, D.Y.; Boldyrev, A.I. Revealing Intuitively Assessable Chemical Bonding Patterns in Organic Aromatic Molecules via Adaptive Natural Density Partitioning. *J. Org. Chem.* **2008**, *73*, 9251–9258. [[CrossRef](#)]
80. Wiberg, K.B. Application of the Pople-Santry-Segal CNDO Method to the Cyclopropylcarbinyl and Cyclobutyl Cation and to Bicyclobutane. *Tetrahedron* **1968**, *24*, 1083–1096. [[CrossRef](#)]
81. Schleyer, P.v.R.; Maerker, C.; Dransfeld, A.; Jiao, H.; van Eikema Hommes, N.J.R. Nucleus-Independent Chemical Shifts: A Simple and Efficient Aromaticity Probe. *J. Am. Chem. Soc.* **1996**, *118*, 6317–6318. [[CrossRef](#)]
82. Richard, F.W. *Bader Atoms in Molecules. A Quantum Theory*; Oxford University Press: Oxford, UK, 1990; ISBN 9780198558651.
83. Becke, A.D.; Edgecombe, K.E. A Simple Measure of Electron Localization in Atomic and Molecular Systems. *J. Chem. Phys.* **1990**, *92*, 5397–5403. [[CrossRef](#)]
84. Frisch, M.J.; Trucks, G.W.; Schlegel, H.B.; Scuseria, G.E.; Robb, M.A.; Cheeseman, J.R.; Scalmani, G.; Barone, V.; Petersson, G.A.; Nakatsuji, H.; et al. *Gaussian 16 Revision B.01*; Gaussian Inc.: Wallingford, CT, USA, 2016.
85. Schlegel, H.B.; Millam, J.M.; Iyengar, S.S.; Voth, G.A.; Daniels, A.D.; Scuseria, G.E.; Frisch, M.J. Ab Initio Molecular Dynamics: Propagating the Density Matrix with Gaussian Orbitals. *J. Chem. Phys.* **2001**, *114*, 9758–9763. [[CrossRef](#)]
86. Lu, T.; Chen, F. Multiwfn: A Multifunctional Wavefunction Analyzer. *J. Comput. Chem.* **2012**, *33*, 580–592. [[CrossRef](#)] [[PubMed](#)]

Disclaimer/Publisher's Note: The statements, opinions and data contained in all publications are solely those of the individual author(s) and contributor(s) and not of MDPI and/or the editor(s). MDPI and/or the editor(s) disclaim responsibility for any injury to people or property resulting from any ideas, methods, instructions or products referred to in the content.